ELSEVIER

Applied Surface Science 136 (1998) 221–229

applied surface science

Chemical reactivity of $CdCl_2$ wet-deposited on CdTe films studied by X-ray photoelectron spectroscopy

David W. Niles *, Donna Waters, Doug Rose

National Renewable Energy Laboratory, 1617 Cole Boulevard, Golden, CO 80401, USA

Received 5 April 1998; accepted 14 June 1998

Abstract

The authors use X-ray photoelectron spectroscopy to investigate the chemical reactivity of CdTe films exposed to a solution of $CdCl_2$ dissolved in methanol. They show that annealing in vacuum does not instigate a chemical reaction between $CdCl_2$ and CdTe, but that annealing in either $He:O_2$ or pure He leads to the formation of a surface Cl residue comprising Cd, Te, Cl, and O in the form of oxides and oxychlorides. From detailed analysis of X-ray photoelectron data, they propose that CdO, TeO_2, $TeCl_2O$ are building blocks for the surface Cl residue.

PACS: 81.65.−b (surface treatments); 82.65.−i (surface chemistry); 82.80.Pv (X-ray photoelectron spectroscopy); 84.60.Jt (photovoltaic conversion)

Keywords: CdTe; CdO; TeO_2; $CdTeO_3$; $CdCl_2$; Surface chemistry; X-ray photoelectron spectroscopy; Photovoltaic; Solar cells

1. Introduction

Thin-film CdTe is a promising material for photovoltaic energy conversion being developed at the National Renewable Energy Laboratory (NREL) [1]. Several recent review articles on the physics and status of CdTe photovoltaic devices have appeared [2,3]. Among the strengths of CdTe are high photovoltaic energy conversion and ease of manufacturing [4,5].

The stack sequence for a CdTe solar cell is glass/SnO_2/n-CdS/p-CdTe/back contact. The so-called $CdCl_2$ treatment has become a standard, critical processing step in fabricating high-efficiency CdTe-based photovoltaic devices. The wet $CdCl_2$ treatment, applied after deposition of the CdTe absorber layer and prior to the application of a back contact, consists of soaking the CdTe films in methanol containing dissolved $CdCl_2$ and then heating. The vapor $CdCl_2$ treatment involves evaporating $CdCl_2$ on CdTe and then heating [6]. Numerous recent manuscripts show the improvement in CdTe device performance brought about by the $CdCl_2$ treatment [7–11].

A complete model for the effects of the $CdCl_2$ treatment has not evolved. Solar cells are minority-carrier devices, and Cl_{Te} defects should – from

* Corresponding author. Hewlett-Packard, 3404 East Harmony Road, MS 64 Fort Collins, CO 80528-9599, USA. Tel.: +1-970-898-9237; Fax: +1-970-898-6722; E-mail: david_niles@hp.com

0169-4332/98/$ - see front matter
PII: S0169-4332(98)00340-7

simple electron counting – be donors. Park and Chadi have shown that a shallow donor state for Cl_{Te} defects is energetically favorable to the formation of DX centers [12]. Castaldini et al. have enumerated 12 defect trap levels for Cl dopants in CdTe and have shown the importance of the A center and midgap traps [13]. Valdna et al. have shown that $(Te_i^{2-}–Cl_{Te}^{+})^{-}$ and/or $(V_{Cd}^{2-}–Cl_{Te}^{+})^{-}$ shallow acceptor complexes stabilize high p-type conductivity of CdTe films [14]. Loginov et al. have shown that the $CdCl_2$ treatment improves the microstucture of the CdTe films and eliminates active states at the CdS/CdTe interface, presumably by interdiffusion, thereby changing the current transport mechanism [15]. Bayhen and Erçelebi have demonstrated that the electron transport mechanism is dominated by recombination at the CdS/CdTe interface prior to the $CdCl_2$ treatment, and by depletion-region recombination after the treatment [7]. Tousková et al. have shown that grain size does not affect depletion-region recombination [11].

Despite the abundance of studies on microstructure, defects, and device performance, we have found no studies of a chemical nature in the literature. The purpose of these experiments was to add to our knowledge of the $CdCl_2$ treatment by studying chemical reactivity between $CdCl_2$, CdTe, and the native oxide to CdTe. A simple question summarized our purpose: how do the $CdCl_2$ and the CdTe interact chemically during the $CdCl_2$ treatment? Answering this question is basic to the overall understanding of the $CdCl_2$ treatment and the development of a model for how the $CdCl_2$ treatment improves device performance. Furthermore, NREL's baseline process involves an etch in nitric–phosphoric acids to form a p-type Te layer on the back surface before application of a back contact [1,16,17]. This etch also removes the Cl residue. The development of an all-dry, in-line fabrication process mandates eliminating the etch, possibly leaving a Cl-based residue to affect device performance [16].

2. Experiment

CdTe films were deposited to a thickness of 9 μm using close-spaced sublimation in a 0.5 Torr oxygen, 14.5 Torr He ambient at 620°C. The substrate used for the CdTe films was Corning 7059 glass with approximately 1 μm of F-doped SnO_2, 200 nm undoped SnO_2, and 90 nm CdS. The SnO_2 films were made by chemical vapor deposition, and the CdS films were made by chemical-bath deposition. The deposition of the CdTe and CdS films is described in greater detail elsewhere [1].

We chose to limit our study to the wet $CdCl_2$ treatment because that is currently NREL's baseline process for making the most-efficient solar cells. We dipped three CdTe films solution of $CdCl_2$ in methanol at 60°C for 15 min (1.13 g $CdCl_2$ in 100 ml methanol, or 75% saturation). The films were then removed from solution and blown dry with N_2. The first sample was a baseline for these experiments and did not receive a device anneal. The second two samples received device anneals in a tube furnace at 400°C for 30 min in a flowing He:O_2 mixture (100 sccm He and 25 sccm O_2) and pure He, respectively, at atmospheric pressure. For brevity and clarity, we will refer to the He:O_2 mixture as simple O_2. These two gases represent an inert environment (He) and an oxidizing one (O_2). The samples were removed from the oven and transported in air.

We inserted the unannealed CdTe film into a system for X-ray photoelectron spectroscopy (XPS), and annealed in 50°C increments in vacuum while monitoring for chemical reactivity. To provide a baseline for data interpretation, we also studied the temperature behavior of single-crystal CdTe that had been oxidized with ozone. We performed similar annealing experiments for the two samples that received the 400°C device anneals. The XPS system was a commercial Physical Electronics 5600 equipped with a monochromated Al Kα source and a hemispherical analyzer [18]. The energy resolution of our XPS system for high-resolution core line scans was set to 0.2 eV. The spot size was 0.8 mm. We used standard sensitivity factors for our analyzer to determine surface atomic concentrations [18].

A Eurotherm temperature controller coupled to a Kepco power supply supplied power to heat the analysis stage. Although temperature stability of our sample stage is better than 1°C, the temperature tended to overshoot by ~5°C at temperatures below several hundred degrees Celsius. We maintained the samples at the elevated temperature for 5 min, and

then let them cool radiatively before data acquisition. For depth profiles, we sputtered with 1 keV Ar^+ ions at a sputter rate of ~ 1 nm/min.

3. Results and discussion

The growth method outlined in Section 2 produced uniform CdTe films with a typical grain size of several microns and comparable surface roughness. The films are stoichiometric and have the native surface oxide from exposure to air. The $CdCl_2$ residue is known to cover the surface but have a non-uniform thickness. Our X-ray beam averages many grain surfaces.

Fig. 1 shows the Cd $3d_{5/2}$ emission for the sample that did not have the 400°C device anneal as a function of annealing temperature in vacuum. One can identify two distinct components to the Cd $3d_{5/2}$ emission: one consistent with $CdCl_2$ and one consistent with CdTe. For both these compounds, Cd has a nominal valence of $+2$. With increasing temperature, the $CdCl_2$ component of the Cd $3d_{5/2}$ emission attenuates. Fig. 2 shows in detail the Cd 3d emission after annealing in vacuum to 300°C, decomposing the emission into the $CdCl_2$ and CdTe parts. The

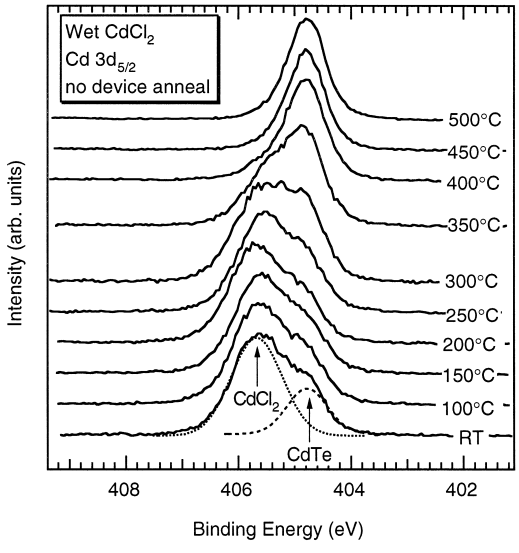

Fig. 1. Cd $3d_{5/2}$ photoelectron signal as a function of vacuum annealing temperature for the sample that did not receive a 400°C device anneal.

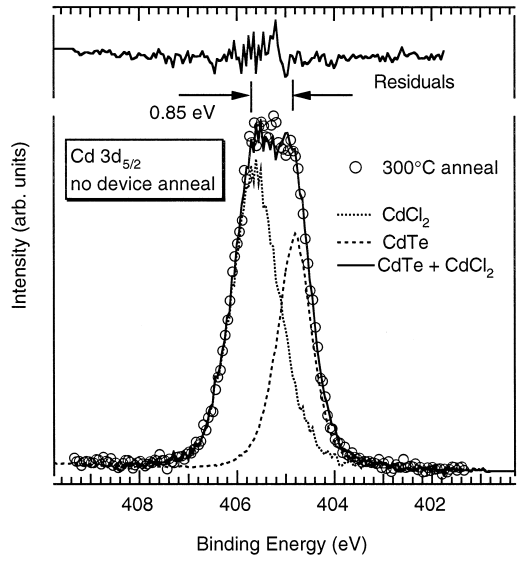

Fig. 2. Cd $3d_{5/2}$ photoelectron spectrum decomposed into its $CdCl_2$ and CdTe signals.

dashed lines do not represent fits, but are spectra taken from a CdTe film that had not been exposed to $CdCl_2$ and a thick $CdCl_2$ film deposited on a glass substrate. The circles are the spectrum also shown in Fig. 1, and the solid line is the sum of the CdTe and $CdCl_2$ signals. The separation in energy between the $CdCl_2$ and CdTe components is 0.85 eV. To a very good approximation, the spectrum from the $CdCl_2$-coated CdTe film is simply a sum of the individual spectra. This result is strong evidence for a lack of chemical interaction between the $CdCl_2$ film and the underlying CdTe film.

Fig. 3 shows emission from the O 1s core level for the sample that did not have the 400°C device anneal as a function of annealing temperature in vacuum. For the room-temperature case, one can see two distinct components to the O 1s emission. The component at higher binding energy, $E_B = 532.3$ eV, is from residual $(OH)^-$ in the film, most likely from the CH_3OH used to dissolve the $CdCl_2$ and air exposure. The intensity in this component attenuates with annealing temperature.

The component at lower binding energy, $E_B = 530.2$ eV, stems from the native CdTe oxide, as we proved by comparison with data from the ozone-oxidized single-crystal CdTe. In the literature, one

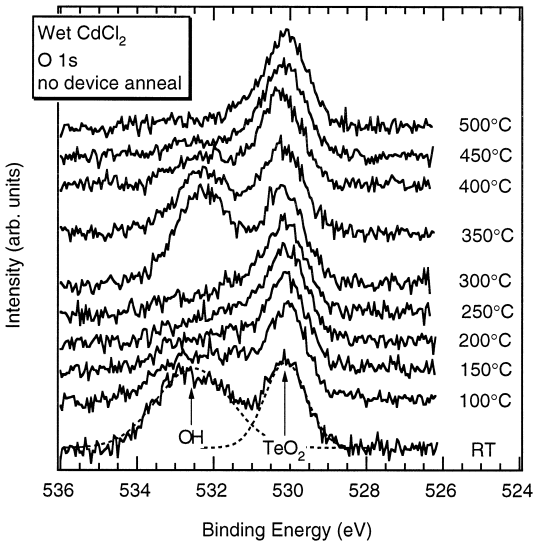

Fig. 3. O 1s photoelectron signal as a function of vacuum annealing temperature for the sample that did not receive a 400°C device anneal.

can find different interpretations for the native CdTe oxide, including $CdTeO_3$, $CdTe_2O_5$, CdO, and TeO_2 [19–22]. Because $CdTeO_3 = CdO + TeO_2$ from atom counting, we contend that one may think of the non-crystalline surface oxide as composed of CdO and TeO_2 building blocks. For these oxides, the Cd, Te, and O valences should be $+2$, $+4$, and -2, respectively.

The Cd $3d_{5/2}$, Te $3d_{5/2}$, and O 1s lines for our ozone-treated CdTe single-crystal were sharp, and the atomic concentrations were Cd = 24 at%, Te = 21 at%, and O = 55 at%. Although one may argue from these data that the ozone-treated CdTe single-crystal surface was consistent with $CdTeO_3$, we will refer this non-crystalline surface as comprising CdO and TeO_2 building blocks to be consistent with later discussion. At 300°C, a third component to the O 1s at $E_B = 531.9$ eV appears as in Fig. 3. We suspect this represents CH_3OH originally trapped in the bulk of the CdTe film but liberated by the 300°C treatment.

For brevity, we do not show the intensity in the Te $3d_{5/2}$ and the Cl 2p as functions of the annealing temperature in vacuum. The Te $3d_{5/2}$ has a main peak at $E_B = 572.2$ eV coming from CdTe (Te with a valence of -2), and an oxide component at $E_B =$ 575.9 eV coming from TeO_2 (Te with a valence of $+4$). Aside from a small decrease in the TeO_2 component, there is little change in either of these two line shapes as a function of vacuum annealing temperature. The Cl 2p shows one chemical component and does not change with annealing temperature.

Fig. 4 shows the atomic concentrations at the surface for Cd, Te, O, and Cl as functions of the vacuum annealing temperature. We have ignored the C 1s signal from adventitious carbon and methanol because carbon is not involved in the chemistry of the interface. We have also decomposed the Cd $3d_{5/2}$ signal into its $CdCl_2$ and CdTe components, the Te $3d_{5/2}$ into its CdTe and TeO_2 components, and used standard sensitivity factors for our XPS system to determine the atomic concentration [18]. The accuracy of the standard sensitivity factors is not better than several atomic percent. The temperature behavior is consistent with a layer of $CdCl_2$ not chemically bound to the underlying CdTe film. The $CdCl_2$ sublimes from the surface congruently, without interacting with the CdTe substrate, leaving a residue-free surface.

Line shapes and atomic concentrations as functions of the vacuum annealing temperature for the

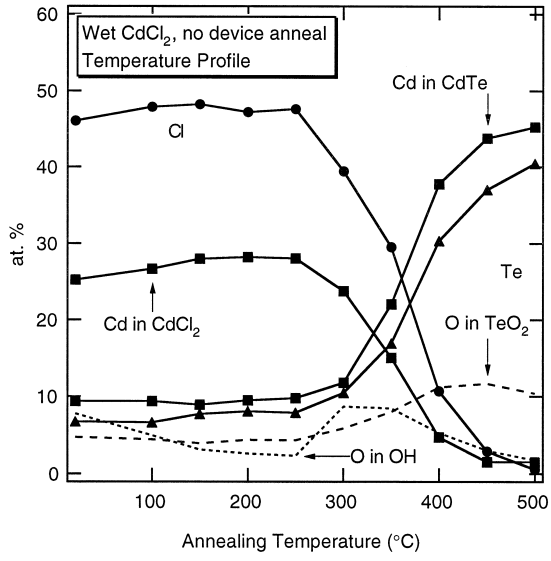

Fig. 4. Atomic concentrations as a function of vacuum annealing temperature for the sample that did not receive a 400°C device anneal.

Table 1
Atomic concentrations after 500°C anneal in vacuum

Sample	Cd	Te	Cl	O
No device anneal	48.2	40.5	0.3	11.1
400°C in O_2	22.0	8.7	2.3	66.9
400°C in He	29.2	19.7	5.5	45.7

samples that had received the 400°C device anneals in O_2 and He did not show any change up to 500°C. In Table 1, we tabulate the atomic concentrations of the surfaces for each of the three samples after they had been annealed in vacuum to 500°C. Whereas the $CdCl_2$ sublimed from the sample that did not have a device anneal, 2 to 5 at.% Cl remain on the samples that had received the 400°C device anneals. This is our primary evidence of a chemical reaction, brought about by the 400°C device anneals in O_2 and He, that binds some Cl to the surface region. One can also see from Table 1 a large increase in O at the surfaces of the samples that had the device anneals. The sample annealed in He has 45.7 at% O. This O may come from residual O_2 in the He gas, the TeO_2 surface oxide, O diffusion from the bulk, and CH_3OH from the solution. The concurrence of O and Cl lead us to believe that O is involved with the chemical reaction that binds the Cl to the surface.

We performed depth profiles to determine the extent of the Cl in the CdTe films. The results appear in Table 2. For the sample that received the 400°C device anneal in O_2, the Cl is near the detection limit after 8 nm. Secondary-ion mass spectrometry has shown that Cl extends throughout the CdTe films [23]. The O persists a little longer than the Cl, but also attenuates. For the sample that received the 400°C device anneal in He, the Cl and O signals persist somewhat longer. In fact, the Cl seems to have reached a stable concentration of 0.8 at% in the bulk of the CdTe film, although more-extensive depth profiles would be required to confirm this result. The O signal also attenuates, but not as rapidly with depth as the Cl signal. For both samples that received the device anneals, the preponderance of the Cl atoms resides in the first 2 to 4 nm of the surface, whereas the O atoms extend ~10 nm deeper into the CdTe films.

Table 2
Depth profiles

Depth	400°C in O				400°C in He			
	Cd	Te	Cl	O	Cd	Te	Cl	O
Surface	22.1	7.8	5.5	64.6	29.6	19.4	5.3	45.7
2 nm	28.7	14.6	1.4	55.3	38.8	23.8	3.1	34.3
4 nm	39.9	32.6	0.4	27.2	44.4	30.8	1.4	23.4
8 nm	50.2	44.8	< 0.2	4.7	48.7	39.9	0.8	10.5
24 nm	–	–	–	–	49.4	40.2	0.9	9.4

The chemistry of the Cd–Te–O–Cl residue present on the surfaces of samples that had received the 400°C device anneals is not straightforward, despite some clear evidence for the compounds that form. Because we have found it awkward to describe the data then propose a model, we have chosen to propose building blocks for these surfaces, determined from the observed valences on each of the elements and the literature, and then show the extent to which the XPS data support the assumed compounds. Fig. 5 shows the compounds that we believe form on the surfaces.

Oxygen is formally more electronegative than chlorine. Any compounds containing Cl–O bonds, such as chlorates and perchlorates, would leave the Cl with a net positive valence, causing the Cl 2p shift by several electron volts to lower binding energy [18]. We eliminate the possibility of Cl–O bonds because we do not observe emission corresponding to Cl with a positive valence. Fig. 6 shows

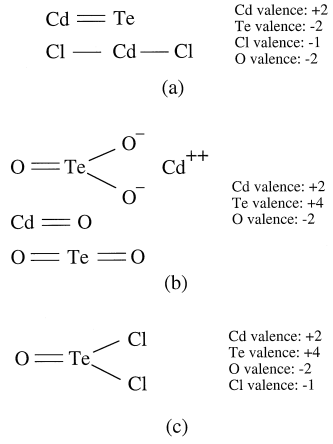

Fig. 5. Assumed molecular building blocks for the surface Cd–Te–O–Cl complex of the samples that received the 400°C device anneals.

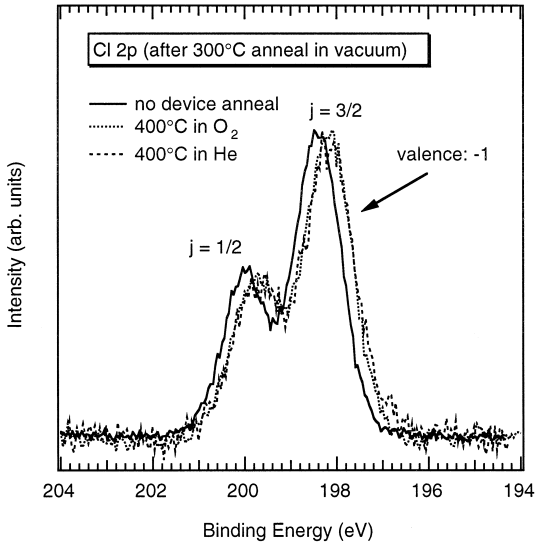

Fig. 6. Cl 2p photoelectron spectra for the three samples after annealing to 300°C in vacuum.

emission from the Cl 2p core level, a doublet with $j = 3/2$ and $j = 1/2$ components. Although we show a narrow window, in a wider window one can see the absence of Cl with a positive valence. Two other compounds one may propose are carbonates and hydroxides. We did not observe any C–O bonds in the C 1s emission, and eliminate carbonates as a possibility. To our misfortune, we can only infer the presence of hydroxides because XPS is insensitive to hydrogen. Hydroxides are generally not stable at elevated temperature, and we will presume that they are not major constituents of the surface residue. A final possibility $TeCl_4$, but this molecule forms a gas at the temperatures used in these experiments [24].

Using the above guidelines, we have constructed several simple molecules consistent with the valences we observe. Fig. 5(a) shows CdTe and $CdCl_2$ molecules; Fig. 5(b) shows a planar representation of the $CdTeO_3$ structure, decomposing into TeO_2 and CdO molecules; and Fig. 5(c) shows a planar representation of a tellurium oxychloride ($TeCl_2O$) molecule [24]. Although the solid form of tellurium oxychloride is $Te_6Cl_2O_{11}$, simple atom counting requires that $Te_6Cl_2O_{11} = TeCl_2O + 5TeO_2$ and validates our assumption of the molecule $TeCl_2O$ as a possible building block. We propose that these molecules are the essential building blocks for the three samples we investigated for this study. The surface region of the sample that did not have the 400°C device anneal comprises CdTe and $CdCl_2$, with relatively little CdO and TeO_2. Annealing in the He environment promoted the formation of $TeCl_2O$ but relatively little CdO, and annealing in the O_2 environment promoted the formation of $TeCl_2O$ and CdO.

Fig. 7 shows the Te $3d_{5/2}$ emission for the three samples and the clear separation between the $+4$ and -2 valence states. The sample that did not receive the 400°C device anneal has only a small $+4$ valence state, meaning only a small amount of TeO_2. Performing the device anneal in O_2 gives a much larger $+4$ state consistent with the formation of more TeO_2, but annealing in He gives approximately twice as much of the $+4$ state as the annealing in O. Table 1 adds to the contradiction by showing that the O_2-annealed sample has 66.9 at% O, whereas the He-annealed sample has 45.7 at% O. The presence of $TeCl_2O$ resolves this contradiction if we assume that binding energy of the Te $3d_{5/2}$ in the $+4$ valence states of TeO_2 and $TeCl_2O$ are equal. Therefore, both device-annealed samples contain TeO_2 and $TeCl_2O$, but the He-annealed sample has twice as much Cl as the O_2-annealed sample (cf. Table 1) and, therefore, twice as much of the oxychloride.

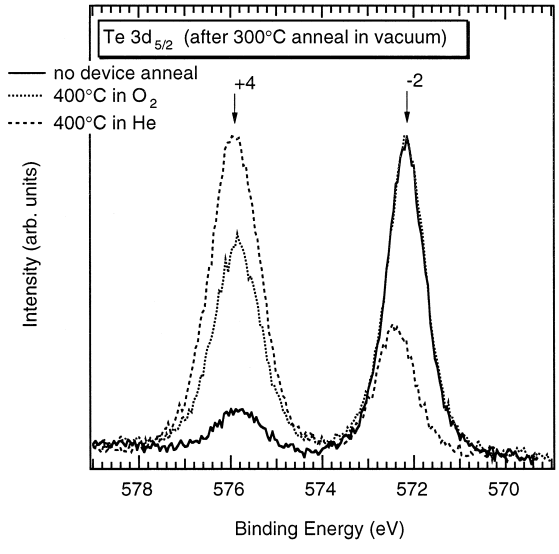

Fig. 7. Te $3d_{5/2}$ photoelectron spectra for the three samples after annealing to 300°C in vacuum.

From the Te $3d_{5/2}$ and Cl 2p emissions that we have just discussed, we have concluded that Te–Cl bonds account for Cl on the surfaces that received the 400°C device anneals. We must then find another compound to account for the added O in the sample annealed in O_2 compared to He. To this end, we will now discuss the O 1s and Cd $3d_{5/2}$ emissions.

The O 1s emission for the three samples shows that CdO can account for the added O in the O_2-annealed sample (Fig. 8). The O 1s has a component at $E_B = 530.2$ eV for all three samples. For the sample that did not receive the device anneal, we also see a component at $E_B = 532.4$ eV, but we argued from the temperature behavior in Fig. 3 that this is just $(OH)^-$ from the CH_3OH solution used to dissolve the $CdCl_2$. The peak at $E_B = 530.2$ eV represents TeO_2.

The samples that received the device anneals in O_2 and He also have the O 1s peak at $E_B = 530.2$ eV. We presume that this peak comes from both TeO_2 and the lone O on the oxychloride shown in Fig. 5(c). Line shapes of the O 1s and Te $3d_{5/2}$ from the depth profiles not shown here support this picture. The O 1s peak at $E_B = 530.2$ eV diminished congruently with the Cl 2p signal and the +4 valence-state signal of the Te $3d_{5/2}$.

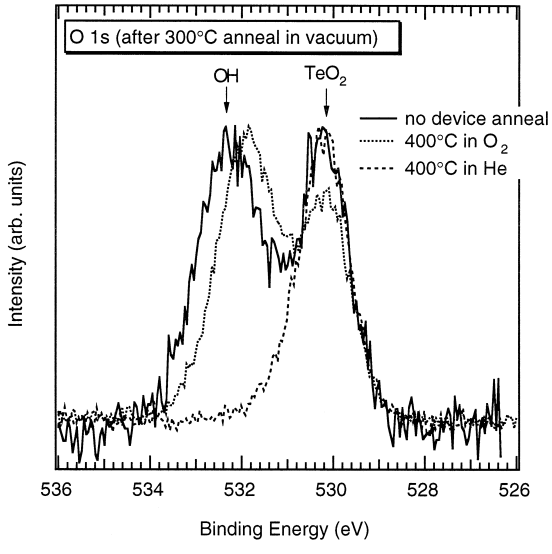

Fig. 8. O 1s photoelectron spectra for the three samples after annealing to 300°C in vacuum.

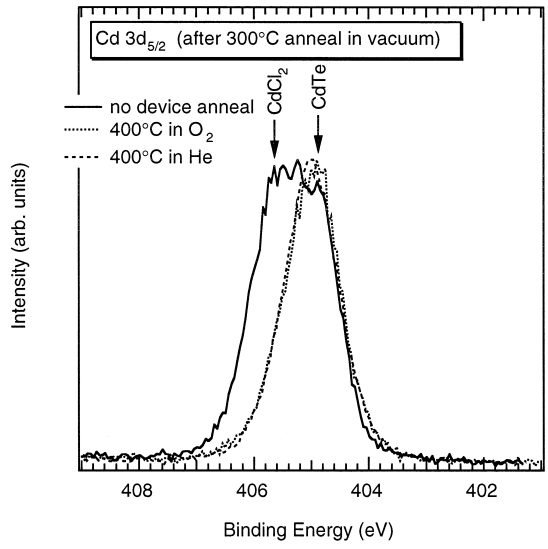

Fig. 9. Cd $3d_{5/2}$ photoelectron spectra for the three samples after annealing to 300°C in vacuum.

The sample that received the 400°C device anneal in O_2 has a second peak on the O 1s at $E_B = 531.9$ eV not present in the sample that received the device anneal in He. Let us presume that this component represents CdO, as supported by the tabulation by Farrow et al. [19]. As one can see in Table 1, the larger concentration of O for the sample that received the 400°C device anneal in O_2 is consistent with the presence of CdO.

From the O 1s emission, we argue for the presence of CdO to account for the addition O on the samples that received the 400°C device anneal in O_2. We will now turn to the Cd $3d_{5/2}$ emission to look for support for this conclusion. Fig. 9 shows a comparison of the Cd $3d_{5/2}$ emission for the three samples. We do not observe Cd consistent with $CdCl_2$, demonstrating once again that the device anneals have removed the $CdCl_2$ (but left Cl behind). The 400°C anneal in O and the 400°C anneal in He appear to result in identical Cd $3d_{5/2}$ emission. The Cd signal from these samples might appear similar to the Cd signal from CdTe, but as shown in more detail in Fig. 10, it is more complicated. The solid line in Fig. 10 is the Cd $3d_{5/2}$ emission taken for the sample that received the He device anneal, after annealing in the vacuum system to 300°C. The dashed line to lower binding energy is the Cd $3d_{5/2}$ emis-

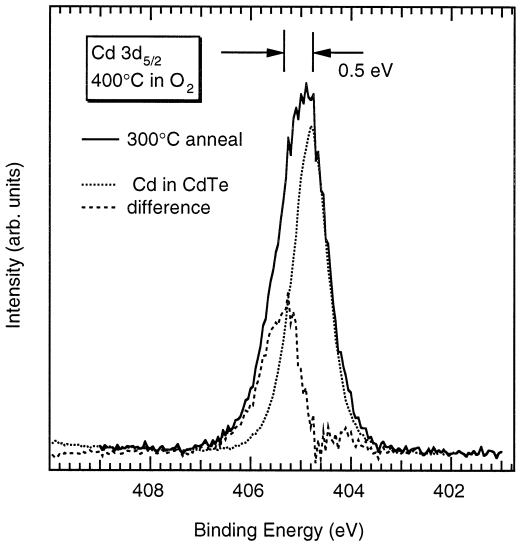

Fig. 10. Detail of the Cd $3d_{5/2}$ spectra showing evidence for Cd–O bonds.

sion taken from a CdTe standard. After the device anneals, the Cd $3d_{5/2}$ emission has two components, one representing CdTe at $E_B = 404.8$ eV and a second one at $E_B = 405.3$ eV.

The appearance of this second peak supports our assumption of CdO being present after the device anneals. However, the binding-energy difference between the O 1s and the Cd $3d_{5/2}$ is $\Delta = 124.3$ eV for CdO and $\Delta = 126.1$ eV for $Cd(OH)_2$ [25]. Subtracting these two deltas from the O 1s peak $E_B = 531.9$ eV gives expected binding energies of $E_B = 531.9 - 124.3$ eV $= 407.6$ eV for CdO and $E_B = 531.9 - 126.1$ eV $= 405.8$ eV for $Cd(OH)_2$. Although not a perfect match, the position of the peak is closer to the expected value for $Cd(OH)_2$ than for CdO.

Our assumption that hydroxides are not a major constituent of the surface residue was based on the instability of hydroxides at elevated temperature and might appear to be in error. However, we would like to reiterate that we contend that the molecules in Fig. 5 represent building blocks of the compounds that form on the device-annealed samples. In reality, the surface residue comprises a complex mixture of Cd, Te, O, and Cl, and the specific bonding arrangement of the Cd atoms is not equal to that of bulk CdO or $Cd(OH)_2$.

4. Conclusions

We draw four fundamental conclusions from our XPS data: (1) soaking a CdTe film in $CdCl_2$ dissolved in methanol does not result in chemical activity at the CdTe surface, (2) annealing to 400°C in either inert or oxidizing environments promotes the formation of a surface layer containing a chemically bonded Cl residue, (3) annealing in an inert environment leads to the formation of Cl–Te bonds in the form of Te oxychlorides, and (4) annealing in an oxidizing environment leads to the formation of Cd–O in the form of cadmium oxide in addition to the tellurium oxychloride.

Analysis of the Cl residue on the CdTe surface is important because it provides insight into the chemical reactions that occur during the $CdCl_2$ treatment. We have described the condition of grain boundaries in at least a portion of the CdTe film and the back surface prior to formation of the back contact. Other $CdCl_2$ treatments may not leave a Cl residue [26]. NREL's current baseline process for solar cell fabrication involves an acid etch after the $CdCl_2$-treatment to prepare for back-contact application [17]. Although possibly mitigating the need to understand the Cl residue, this etch greatly increases the manufacturing costs. Other back-contact processes, such as Te evaporation rather than etching, may leave the Cl residue intact [16].

Acknowledgements

DOE Contract No. DE-AC36-83CH11093 supported this work. The authors thank Y. Mahathongdy and D. Albin of NREL for assistance with the $CdCl_2$ depositions and for supplying a $CdCl_2$ source plate for comparison. DWN sincerely thanks J. Turner and D. King of NREL for sharing their expertise in advanced inorganic chemistry.

References

[1] D.H. Rose, D.S. Albin, R.J. Matson, A.B. Swartzlander, X. Li, R.G. Dhere, S. Asher, F.S. Hasoon, P. Sheldon, Mater. Res. Soc. Proc. 426 (1996) 337.

[2] A.W. Brinkman, in: P. Capper (Ed.), Narrow Gap II–VI Compounds for Optoelectronic and Electromagnetic Applications, Chapman and Hall, UK, 1998, p. 526.
[3] P.V. Meyers, R.W. Birkmire, Prog. Photovoltaics 3 (1995) 393.
[4] M.A. Green, K. Emery, K. Bücher, D.L. King, S. Igari, Prog. Photovoltaics 5 (1997) 265.
[5] S. Kumazawa, S. Shibutani, T. Nishio, T. Aramoto, H. Higuchi, T. Arita, A. Hanafusa, K. Omura, M. Murozono, H. Takakura, Solar Energy Materials and Solar Cells 49 (1997) 205, and references therein.
[6] T.X. Zhou, N. Reiter, R.C. Powell, R. Sasala, P.V. Meyers, Proc. Twenty-Fourth IEEE Photovoltaics Specialists Conf., Waikoloa, HI 1994, p. 103.
[7] H. Bayhen, C. Erçelebi, Semi. Sci. Technol. 12 (1997) 600.
[8] M.A. Lourenço, Y.K. Yew, K.P. Homewood, K. Durose, H. Richter, D. Bonnet, J. Appl. Phys. 82 (1997) 1423.
[9] A. Kampmann, D. Lincot, J. Elect. Chem. 418 (1996) 73.
[10] B.E. McCandless, L.V. Moulton, R.W. Birkmire, Prog. Photovoltaics 5 (1997) 249.
[11] J. Tousková, D. Kindl, J. Tousek, Thin Solid Films 293 (1997) 272.
[12] C.H. Park, D.J. Chadi, Phys. Rev. B 52 (1995) 11884.
[13] A. Castaldini, A. Carallini, B. Faboni, P. Fernandez, J. Piqueras, J. Appl. Phys. 83 (1998) 2121.
[14] V. Valdna, F. Buschmann, E. Mellikov, J. Cryst. Growth 161 (1996) 164.
[15] Y.Y. Loginov, K. Durose, A. Allak, H.M. Galloway, S.A. Oktik, S. Brinkman, A.W. Richter, D. Bonnet, J. Cryst. Growth 161 (1996) 159.
[16] D.W. Niles, X. Li, D. Albin, D. Rose, T. Gessert, P. Sheldon, Prog. Photovoltaics 4 (1996) 225.
[17] D.W. Niles, X. Li, P. Sheldon, H. Höchst, J. Appl. Phys. 77 (1995) 4489.
[18] Handbook of X-ray Photoelectron Spectroscopy, in: Jill Chastain (Ed.), Physical Electronics, Eden Prairie, 1992.
[19] R.F.C. Farrow, P.N.J. Dennis, H.E. Bishop, N.R. Smart, J.T.M. Wotherspoon, Thin Solid Films 88 (1982) 87.
[20] A.B. Christie, I. Sutherland, J.M. Walls, Surf. Sci. 135 (1983) 225.
[21] F. Wang, A. Schwartzman, A.L. Fahrenbruch, R. Sinclair, R.H. Bube, C.M. Stahle, J. Appl. Phys. 62 (1987) 1469.
[22] A. Zapata-Navarro, P. Bartolo-Pérez, M. Zapata-Torres, R. Castro-Rodriguez, J.L. Peña, M.H. Farías, J. Vac. Sci. Technol. A 15 (1997) 2537.
[23] R. Dhere, S.E. Asher, K.M. Jones, M.M. Al-Jassim, H.R. Moutinho, R.H. Rose, P. Dippo, AIP Conf. Proc. 353 (1995) 392.
[24] G.H. Westphal, R. Rosenberger, P.R. Cunningham, L.L. Ames, J. Chem. Phys. 72 (1980) 5192.
[25] D.W. Niles, G. Herdt, M. Al-Jassim, J. Appl. Phys. 81 (1997) 1978.
[26] B.E. McCandless, R.W. Birkmire, D.G. Jensen, J.E. Phillips, I. Youm, AIP Proc. 394 (1996) 647.